Probing Diffusion of Single Nanoparticles at Water–Oil Interfaces

*Dapeng Wang, Stoyan Yordanov, Harsha Mohan Paroor, Ashis Mukhopadhyay, Christopher Y. Li, Hans-Jürgen Butt, and Kaloian Koynov**

The diffusion of nanoparticles at a water–alkane interface is studied using fluorescence correlation spectroscopy. Hydrophilic and hydrophobic quantum dots of 5, 8, and 11 nm radius are used. A slow-down of nanoparticle diffusion at the liquid–liquid interface is observed. The effect is most evident when the viscosities of both liquid phases are similar, here, at the water–decane interface. In this case, the interfacial diffusion coefficients of the hydrophilic particles are 1.5 times and those of the hydrophobic particles 2 times lower than the corresponding bulk values.

1. Introduction

The process of small particle adsorption at a liquid–liquid interface has attracted continuous attention ever since its emulsion-stabilizing effect was discovered over a century ago.[1] Nowadays it is obvious that a good understanding of the dynamics and self organization of nanometer-sized objects, e.g., molecules, macromolecules, and nanoparticles (NPs), at immiscible liquid–liquid interfaces is of fundamental significance for soft-matter physics and cell biology. It is also important for a number of technological applications in material synthesis, pharmacy, microfluidics, and nanotechnology. For example, it is essential for the fabrication of novel materials based on 2D- or 3D-ordered NPs with unique optical, magnetic, and electronic properties[2] or for the design of nanosized drug carriers that can deliver drugs through cell membranes.[3]

D. P. Wang, S. Yordanov, H. M. Paroor, Prof. H.-J. Butt, Dr. K. Koynov
Max-Planck Institute for Polymer Research
Ackermannweg 10, 55128 Mainz, Germany
E-mail: koynov@mpip-mainz.mpg.de
Prof. A. Mukhopadhyay
Department of Physics and Astronomy
Wayne State University
Detroit, Michigan 48201, USA
Prof. C. Y. Li
Department of Materials Science and Engineering
Drexel University
Philadelphia 19104, USA

DOI: 10.1002/smll.201101823

Diffusion is an important transport process that often controls self organization. Therefore, it is important to understand the diffusion of adsorbed particles at liquid–liquid interfaces. In answering this question, most research attention was paid to theoretical analysis and computer simulations, due to the limitations of the available experimental techniques. The macroscopic theories developed can notably describe the stability and the interactions of microcolloids at interfaces.[4] Some aspects of the theories may remain valid for NPs, but one could expect new effects, for example, due to the stronger influence of thermal fluctuations at this scale. Furthermore, interesting physics can emerge as the nanoparticle size approaches the length scale of interfacial region.[5] Recently, a molecular dynamics simulation investigated the interaction between NPs and ideal liquid–liquid interfaces and predicted that it may be stronger than the estimate from classical theory.[6] It is, therefore, very important to explore experimentally the dynamics of single NPs at real interfaces.

Unfortunately, the range of experimental techniques that can be used to study NP diffusion on liquid–liquid interfaces is rather limited. Most notably, optical (fluorescence) microscopy combined with particle tracking has proved useful for addressing the micrometer-sized colloid dynamics on air–liquid and liquid–liquid interfaces.[7] However, this technique cannot be easily applied to NPs or single molecules due to the limitations in both sensitivity and speed that are required to study fast NP diffusion. Alternatively, fluorescence photobleaching techniques can be used to study the diffusion of molecules and nanoparticles at interfaces provided that the surface coverage is high enough.[8] Such a situation, however, is undesirable when the diffusion and drag experienced by individual particles is addressed. High surface coverage may

small NANO MICRO

result in particle–particle interactions or even induce cluster formation due to capillary attraction.[9] Therefore, while the above-mentioned techniques, as well as some other methods,[10] have delivered valuable information on the particle dynamics at liquid interfaces, new, highly sensitive experimental techniques are needed for monitoring nanometer-sized objects with high mobilities at the single-particle level.

In the recent years, the fluorescence-correlation spectroscopy (FCS) has emerged as a powerful tool for investigating the diffusion of fluorescent molecules, macromolecules, or NPs in various environments. The method is based on measuring the fluctuations of the fluorescent light intensity caused by the fluorescent species diffusing through the focus of a confocal microscope. Due to minimal requirements on sample amounts and its high sensitivity and selectivity, FCS has found widespread application, probing quantities such as diffusion coefficients, kinetic rate constants, equilibrium-binding constants, intracellular particle concentrations, viscosity of complex liquids, flow velocities, etc.[11] It was also used to address interfacial phenomena, e.g., the diffusion of synthetic polymers on solid–liquid interfaces, dynamics in model and cell membranes, etc.[12] As compared to other techniques, FCS is well suited for studies of NP diffusion on liquid–liquid interfaces: FCS offers the possibility to monitor nanometer-sized objects with high mobility at a low surface coverage.

In this letter, we present a FCS study of the diffusion of fluorescent semiconductor nanoparticles (quantum dots) at planar water–oil interfaces. The effects of several important parameters, i.e., the particles' size, their surface chemistry (hydrophobic/hydrophilic), and the oil-phase viscosity, were systematically explored. Most notably, a significant decrease of the NP mobility at the interface as compared to the corresponding bulk solutions was observed.

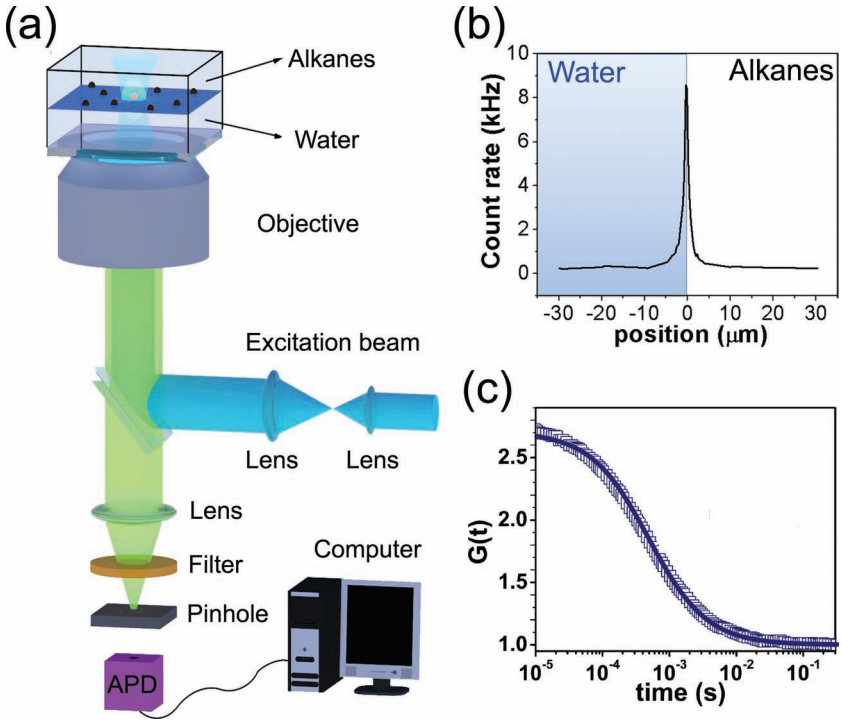

Figure 1. a) Schematic representation of the experimental setup. b) Fluorescence intensity scan through the water–hexane interface with adsorbed $QD_{w\text{-}5}$. The scanning is done by moving the focus from water phase to alkane phase with a step of 200 nm. c) An autocorrelation function of the $QD_{w\text{-}5}$ (open squares) diffusing at water–hexane interface, which can be adequately fitted by equation 2 (solid line).

2. Results and Discussion

The interfacial mobility of four different types of quantum dots (QDs) with various sizes and surface functionalities (see the Supporting Information (SI), Table S1) was studied. Most of them were coated with carboxyl-derivatized amphiphilic molecules that make them easily dispersible in water. In the text below these hydrophilic, water-soluble nanoparticles are referred to as $QD_{w\text{-}j}$ where j indicates their hydrodynamic radius (R_H). For comparison, hydrophobic quantum dots $QD_{o\text{-}j}$ coated with aliphatic hydrocarbons that can be well dispersed in organic solvent, e.g., toluene, chloroform, alkanes, etc., were also studied.

The diffusion coefficients of the QDs at the water–alkane interfaces (D_{2D}) were measured by fluorescence correlation spectroscopy (**Figure 1**a). A laser beam was tightly focused on to the sample by a high-numerical-aperture microscope objective. The excited fluorescence was collected by the same objective and directed to an avalanche photodiode detector (APD). By shifting the objective in vertical direction the position of the focus can be scanned through the sample in 200 nm steps. A typical scan through the water–hexane interface at which $QD_{w\text{-}5}$ are deposited is shown in Figure 1b. A fluorescence signal was detected only when the focus was at the interface. This confirms that the QDs resided at the interface only.

Next the focus was adjusted at the interface and the fluctuations in fluorescence intensity $F(t)$ caused by the lateral diffusion of the QDs were measured and evaluated in terms of an autocorrelation function (equation 1), as shown in Figure 1c:

$$G(t) = \frac{\langle \delta F(t')\delta F(t'+t)\rangle}{\langle F(t')\rangle^2} \quad (1)$$

$$G(t) = \frac{1}{N}\frac{1}{\left[1+\frac{t}{\tau_D}\right]} \quad (2)$$

where N is the average number of diffusing particles in the confocal observation volume. τ_D is the so-called diffusion time that is related to the lateral dimension of the observation volume ω_{xy} and the particle's diffusion coefficient at the interface, through (equation 3):

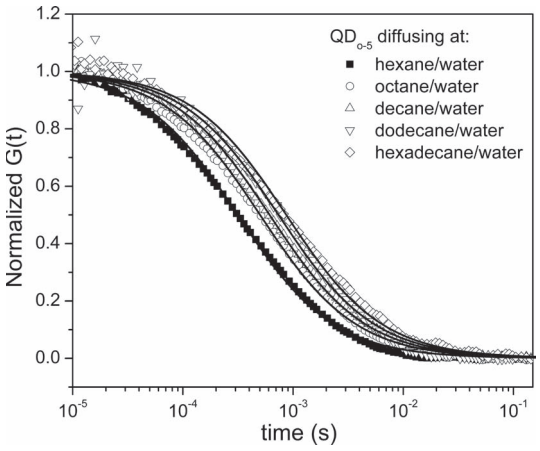

Figure 2. Normalized experimental autocorrelation curve of QD_{o-5} at different water–alkane interfaces (symbols) and the corresponding fits wit equation 2 (solid lines).

$$D_{2D} = \frac{\omega_{xy}^2}{4\tau_D} \quad (3)$$

A fit of this experimental autocorrelation curve with equation 2 (Figure 1c) yields the QDs' diffusion coefficient and their concentration (surface density). Detailed information for the FCS setup and data evaluation procedure is provided in the Experimental Section and the SI.

Figure 2 shows typical normalized FCS autocorrelation curves for QD_{o-5} diffusing at water–alkane interfaces. The experimental autocorrelation curves are adequately represented by equation 2, which confirms that the QDs undergo pure 2D Brownian diffusion. The average diffusion time through the FCS observation volume increased with the viscosity of the alkanes (η_a). This is further illustrated in **Figure 3**, where the diffusion coefficient of QD_{o-5} at water–alkane interfaces, D_{2D}, is plotted versus the viscosity. For comparison, the diffusion coefficient of the same quantum dots measured in bulk alkanes, D_{bulk}, is plotted. The later decreases as $D_{bulk} \sim \eta_a^{-\alpha}$ with $\alpha = 1$, as expected for free 3D Brownian diffusion. At the water–alkane interfaces, the diffusion coefficient decreases less steeply, i.e., $D_{2D} \sim \eta_a^{-\alpha}$ with

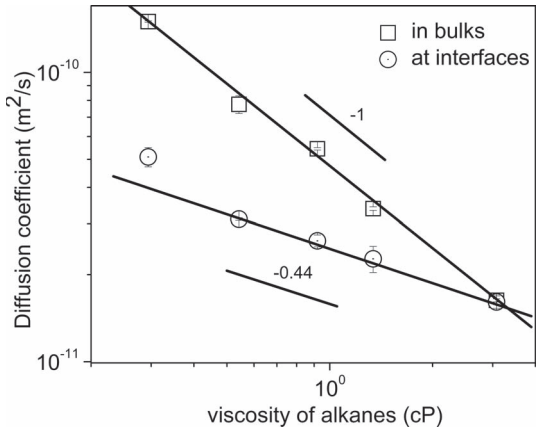

Figure 3. Diffusion coefficient of QD_{0-5} diffusing in bulk and at the corresponding water–alkane interfaces versus viscosity of alkanes.

$\alpha = 0.35$–0.53. This can be attributed to the fact that the QDs are only partially immersed in the alkane phase and are thus only partially affected by its viscosity.

D_{2D} is lower than D_{bulk} in all cases, which implies that the QDs diffuse more slowly when they are at interfaces. This finding cannot be explained merely by viscosity differences between water and alkanes. Indeed the viscosity of the water is higher than that of the alkanes and may lead to a diffusion slowdown only in the case of the short alkanes, e.g., hexane and octane (the first 2 points in Figure 3). The longer alkanes have higher viscosities than the water and thus the partial immersion of the NPs in the water phase should lead to an increase of the diffusion coefficient, which was not observed. For the water–decane interface, the viscosities of both liquids are similar. Nevertheless the diffusion coefficient at this interface is approximately two times smaller than in bulk decane. This effect cannot be explained with classical theories[13] and requires further analysis.

Before further interpretation, it is important to consider (and exclude) some possible artifacts that may lead to an apparent slowdown of interfacial diffusion. For example, a high surface coverage may result in particle–particle interactions or even induce cluster formation, thus influencing (decreasing) the interfacial diffusion. In extreme cases, the particles may self-assemble in a monolayer at the water-oil interfaces. Lin et al. have used fluorescence photobleaching techniques to measure the nanoparticles mobility in such monolayers and found that the in-plane diffusion coefficient of 4.6 nm tri-*n*-octyl-phosphine-oxide covered cadmium selenide nanoparticles is 4 orders of magnitude lower than the diffusion coefficient of the same nanoparticles dispersed in toluene, as measured by dynamic light scattering.[8b] To exclude this effect we prepared samples with a particularly low surface coverage. Furthermore the fits to the FCS autocorrelation curves (Figure 2) provide independent information for the average number of particles in the observation volume and thus for the particle concentration at the interface. Using these fits we estimated that the area per QD in the experiments was approximately 0.2–0.5 μm^2, which is three or four orders of magnitude larger than the cross-section of the QDs. Thus, one should not expect any effects from short-ranged particle–particle interactions. Furthermore the presence of QD clusters (aggregates) should be also excluded as such clusters are easily detected in a FCS experiment by their anomalously high brightness as compared to the individual QDs. In order to get better insight on this effect we have prepared several water–alkane interfaces with different concentrations of the dispersed QDs and measured the nanoparticle interface diffusion. The corresponding FCS autocorrelation curves (SI, Figure S4) show that until certain threshold, the nanoparticles concentration (surface coverage) does not affect the interfacial diffusion. A higher increase of concentration, however, leads to cluster formation and much slower interface diffusion.

Another possible reason for the slowdown of the QDs at the water–alkane interface may be the presence of some unknown solutes possessing a strong surface activity and consequently enriching at the interface.[14] Based on an intuitive understanding, this may hinder the movement of the QDs

small NANO MICRO

Table 1. Interfacial tension of water–alkanes and viscosity of alkanes ($T = 20$ °C)

alkanes	γ[mN m^{-1}][a)]	γ[mN m^{-1}][b)]	viscosity [cP]
hexane	50.80	49.65	0.294
octane	51.64	50.56	0.542
decane	52.33	51.36	0.92
dodecane	52.87	51.69	1.34
hexadecane	-	52.42	3.078
water	-	-	1.002

[a)]In reference [14]; [b)]The interfacial tension was measured by Du-Noüy ring tensiometer. Each value is an average of 10 measurements with statistical error of ±0.05 mN m^{-1}.

by increasing the drag force that they experience and therefore result in a decrease of the QDs diffusion coefficient at the interface. To avoid such effects we took a special care in cleaning the sample cells and the corresponding liquids. Furthermore we have measured the interfacial tension for all water–alkane interfaces by an Du-Noüy ring tensiometer (DCAT 11EC, Data Physics Ltd.) as tabulated in **Table 1**. The obtained values agree with those reported in the literature within the statistical error[15] confirming the purity of our interfaces. Finally we explored in a controlled way how the presence of surfactants influences the interfacial diffusion of the QDs. For that purpose, we added sodium dodecylsulfate with concentration of 10^{-4} M into the aqueous phase before the deposition of $QD_{w\text{-}5}$ and creation of a water-decane interface. This resulted in a continuous increase of D_{2D} over approximately 1 h (reflecting the adsorption of the surfactant molecules on the interface) to a final value much higher than that measured when pure water was used as aqueous phase. In contrast, D_{2D} showed no time dependence in the absence of surfactant. Thus, we believe that the observed slowdown of the QDs at the interface is not affected by adsorption of impurities at the interface.

The behavior of charged NPs trapped at the water–oil interface can be affected by long-range electrostatic interactions.[4e,16] As the overall charge of $QD_{o\text{-}5}$ is not well known and probably small, we proceeded by studying the interfacial diffusion of water dispersible carboxylated QDs that carry a negative charge. Typical examples of experimental autocorrelation curves measured for these QDs that also easily adsorbed at water–alkane interfaces are shown in **Figure 4**. The autocorrelation curves can be adequately fitted by equation 2 yielding the corresponding interface diffusion coefficient, D_{2D}. **Figure 5**a shows D_{2D} versus the viscosity of alkanes for $QD_{o\text{-}5}$ and several carboxylated, water-soluble quantum dots with different sizes, $QD_{W\text{-}j}$. The charged $QD_{W\text{-}5}$ diffuses faster than the weakly (un)charged $QD_{o\text{-}5}$ in spite of their similar sizes. This indicates that electrostatic interactions are not the reason for the slowdown of interfacial diffusion. This was further confirmed by control experiments, showing that D_{2D} of $QD_{W\text{-}11}$ at water–octane interface did not change upon adding a salt (potassium chloride) with concentration of 10^{-2}–10^{-3} M to the water phase.

Another important parameter is the wetting property of the NPs, i.e., the corresponding contact angle. The contact

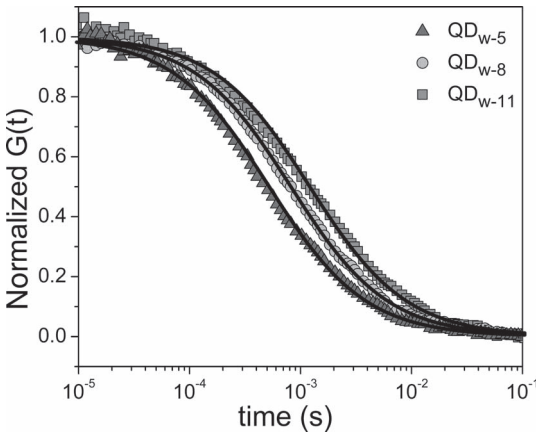

Figure 4. Normalized experimental autocorrelation curves of $QD_{w\text{-}j}$ at water–decane interfaces (symbols) and the corresponding fits wit equation 2 (solid lines).

angle determines their precise position at the interface and thus the drags applied from the water and the oil phases, respectively. To obtain more information on their wetting properties we prepared thin films of QDs (≈50 nm) by solution-casting on glass substrates. The water contact angle on these layers was measured by the sessile drop method. SI, Figure S2 shows that the $QD_{o\text{-}5}$ had a contact angle of 72° whereas the contact angle of all $QD_{W\text{-}j}$ was 8°. Clearly, these values are only estimation for the real contact angle on the QDs. However, combined with the fact that the slope of D_{2D}

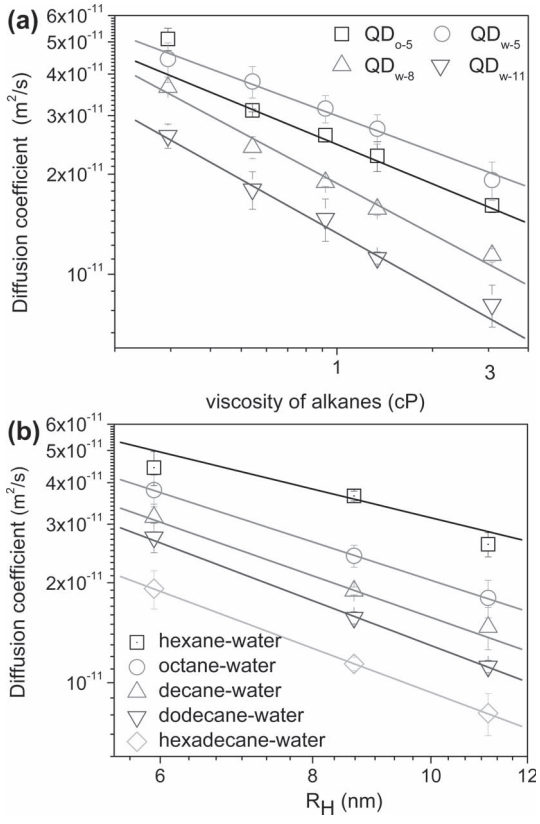

Figure 5. Diffusion coefficients of $QD_{w\text{-}j}$ at the water-alkane interfaces as a function of a) viscosity of alkanes and b) hydrodynamic radii of particles.

Table 2. The constants α/β, deduced from equation 4.

n-alkane	$QD_{w\text{-}5}$	$QD_{w\text{-}8}$	$QD_{w\text{-}11}$
hexane	0.35/0.89	0.51/0.89	0.53/0.89
octane	0.35/1.19	0.51/1.19	0.53/1.19
decane	0.35/1.29	0.51/1.29	0.53/1.29
dodecane	0.35/1.39	0.51/1.39	0.53/1.39
hexadecane	0.35/1.37	0.51/1.37	0.53/1.37

versus η_a for $QD_{o\text{-}5}$ is steeper than that of $QD_{W\text{-}5}$, they suggest that the $QD_{o\text{-}5}$ are positioned more towards the middle of the interface while the $QD_{w\text{-}5}$ are located more in the aqueous phase. Nevertheless, the precise position of the QDs at the water–oil interface is rather uncertain due to the presence of line tension and capillary wave effects.[6] Furthermore, the slope of $D_{2D}(\eta_a)$ changes only slightly with the size of the QDs (Figure 5a). The experimentally measured values of D_{2D} for all studied QDs are summarized in SI, Table S2. The values of the corresponding diffusion coefficients measured in bulk (in water or in decane) are also given for comparison.

The double logarithmic plots (Figure 5) show that the dependence of the interfacial diffusion coefficient on the radius of the QD and on the viscosity of alkanes can be described by a power law according to (equation 4):

$$D_{2D} = a\eta_a^{-\alpha} R_H^{-\beta} \quad (4)$$

Here, α and β are empirical constants. Their values obtained by the fits to the experimental data (Figure 5) are tabulated in **Table 2**. Two conclusions can be drawn: (1) α slightly decreases with increasing R_H; (2) β increases from water-hexane to water-hexadecane interfaces.

The main result of this study is that the NPs diffuse more slowly when they are at an interface than in the bulk. We can only speculate why. In general, when a particle diffuses laterally new interfacial area is created behind it while interfacial area is consumed ahead of it. The gain in energy from the disintegration of interface in front can to a large degree not be used to create new interface behind the particle. Therefore, energy is dissipated. The energy dissipation acts like a friction coefficient and diffusion is slowed down. A possible alternative explanation for the decreased D_{2D} is that the laminar flow of liquid around the particle is different from the Stokes flow since the interface imposes an additional boundary condition. Only for liquids with identical viscosity and a contact angle of 90° Stokes flow should be preserved. In all other cases the flow is different and the effective friction coefficient can increase.[17] Finally the presence of capillary waves[18] may lead to an effectively large interfacial area (particles diffusing up and down along the waves) and give rise to an effectively slower diffusion.

3. Conclusion

The present study demonstrates that the fluorescence correlation spectroscopy is very well suited to address the diffusion of single nanoparticles on planar water-oil interfaces. We used the method to measure the interfacial diffusion coefficient of hydrophilic and hydrophobic quantum dots with sizes in the range 10–20 nm adsorbed at water–alkane interfaces. We found that in all cases the interfacial diffusion coefficient D_{2D}, depends on the particle size and the viscosities of both liquid phases. Furthermore the quantum dots diffuse more slowly when they are at the interface than in the bulk. While the exact mechanism of this slowdown is not clear and demands further investigations, the effect should be considered in all studies and applications for which the dynamics on liquid interfaces is relevant.

4. Experimental Section

Materials: The QDs used in this study were purchased from Invitrogen. As liquids we used a deionized water (miliQ) and series of alkanes purchased from Sigma-Aldrich. The alkanes were further purified by mixing them with water and removing the formed interface as described by Goebel and Lunkenheimer.[14]

Tensiometry: All the interfacial tension measurements reported in this work were done using software controlled Du-Noüy ring tensiometer (DCAT 11EC, Data Physics Ltd.) with ring height = 25 mm, ring diameter = 18.7 mm and wire thickness 0.37 mm. Samples were measured in a 50 cm^3 measuring cell at a temperature 298 ± 0.5 K. The platinum–iridium ring was flame-dried before each experiment. The ring hanging from the balance hook is immersed just below the liquid–liquid interface and is pulled upwards slowly. This cause the denser liquid film to stretch and the maximum force experienced is recorded. This force is directly related with the interfacial tension along with the densities of the liquids.

Deposition of the QDs at the Water–Alkane Interface: First a defined amount (approximately 10 µL) of pure water was added into the measuring cell. Then, 1 µL of QD dispersion with a concentration of ≈10^{-9} M, was dropped upon the pure water. The QDs were allowed to absorb to the interface for typically 2 min. Finally, around 400 µL of alkane was carefully added on top of the water surface.

Fluorescent Correlation Spectroscopy: Commercial FCS setup comprising of the module ConfoCor2 and an inverted microscope (Axiovert 200, Carl Zeiss, Jena, Germany). A 40× Plan Neofluar multi-immersion objective with a numerical aperture of 0.9 and glycerol as immersion liquid were used in this study. The QDs were excited by an Ar+ laser (488 nm), and the emission was collected after filtering with LP530 long pass filter. Each FCS measurement was conducted at five different lateral positions at the interface and it was repeated on a different day with freshly prepared sample. Further information on the FCS setup and data evaluation procedure is provided in the SI.

Supporting Information

Supporting Information is available from the Wiley Online Library or from the author.

Acknowledgements

The financial support by DFG (SPP1259, KO3747/3-1) is gratefully acknowledged. C.Y.L. is grateful to the support of Alexander von Humboldt Foundation and A.M. wants to acknowledge the support of NSF-DMR-0605900.

[1] S. U. Pickering, *J. Chem. Soc.* **1907**, *91*, 307.
[2] a) A. P. Alivisatos, *Endeavour* **1997**, *21*, 56; b) Y. Lin, H. Skaff, T. Emrick, A. D. Dinsmore, T. P. Russell, *Science* **2003**, *299*, 226; c) H. W. Duan, D. Y. Wang, D. G. Kurth, H. Mohwald, *Angew. Chem. Int. Ed.* **2004**, *43*, 5639; d) J. T. Russell, Y. Lin, A. Boker, L. Su, P. Carl, H. Zettl, J. B. He, K. Sill, R. Tangirala, T. Emrick, K. Littrell, P. Thiyagarajan, D. Cookson, A. Fery, Q. Wang, T. P. Russell, *Angew. Chem. Int. Ed.* **2005**, *44*, 2420; e) T. P. Bigioni, X. M. Lin, T. T. Nguyen, E. I. Corwin, T. A. Witten, H. M. Jaeger, *Nat. Mater.* **2006**, *5*, 265; f) F. Bresme, M. Oettel, *J. Phys. Condens. Matter* **2007**, *19*; g) P. Arumugam, D. Patra, B. Samanta, S. S. Agasti, C. Subramani, V. M. Rotello, *J. Am. Chem. Soc.* **2008**, *130*, 10046; h) C. E. McNamee, S. Yamamoto, H. J. Butt, K. Higashitani, *Langmuir* **2011**, *27*, 887.
[3] A. Angelova, B. Angelov, R. Mutafchieva, S. Lesieur, P. Couvreur, *Accounts Chem. Res.* **2011**, *44*, 147.
[4] a) A. Scheludko, B. V. Toshev, D. T. Bojadjiev, *J. Chem. Soc.–Faraday Trans. I* **1976**, *72*, 2815; b) P. Pieranski, *Phys. Rev. Lett.* **1980**, *45*, 569; c) V. N. Paunov, P. A. Kralchevsky, N. D. Denkov, K. Nagayama, *J. Colloid Interface Sci.* **1993**, *157*, 100; d) V. N. Paunov, B. P. Binks, N. P. Ashby, *Langmuir* **2002**, *18*, 6946; e) R. Aveyard, B. P. Binks, J. H. Clint, P. D. I. Fletcher, T. S. Horozov, B. Neumann, V. N. Paunov, J. Annesley, S. W. Botchway, D. Nees, A. W. Parker, A. D. Ward, A. N. Burgess, *Phys. Rev. Lett.* **2002**, 88; f) B. P. Binks, *Curr. Opin. Colloid Interface Sci.* **2002**, *7*, 21.
[5] M. Oettel, S. Dietrich, *Langmuir* **2008**, *24*, 1425.
[6] D. L. Cheung, S. A. F. Bon, *Phys. Rev. Lett.* **2009**, 102.
[7] a) J. Wu, L. L. Dai, *Langmuir* **2007**, *23*, 4324; b) V. Prasad, S. A. Koehler, E. R. Weeks, *Phys. Rev. Lett.* **2006**, 97; c) F. Ortega, H. Ritacco, R. G. Rubio, *Curr. Opin. Colloid Interface Sci.* **2010**, *15*, 237; d) Y. Peng, W. Chen, T. M. Fischer, D. A. Weitz, P. Tong, *J. Fluid Mech.* **2009**, *618*, 243.
[8] a) M. Negishi, H. Seto, M. Hase, K. Yoshikawa, *Langmuir* **2008**, *24*, 8431; b) Y. Lin, A. Boker, H. Skaff, D. Cookson, A. D. Dinsmore, T. Emrick, T. P. Russell, *Langmuir* **2005**, *21*, 191.
[9] a) H. J. Butt, *Science* **2011**, *331*, 868; b) E. Koos, N. Willenbacher, *Science* **2011**, *331*, 897.
[10] A. Stocco, T. Mokhtari, G. Haseloff, A. Erbe, R. Sigel, *Phys. Rev. E* **2011**, 83.
[11] a) R. Rigler, E. Elson, *Fluorescence Correlation Spectroscopy: Theory and Applications*, Springer Verlag, Berlin **2001**; b) E. Haustein, P. Schwille, *Annu. Rev. Biophys. Biomol. Structure* **2007**, *36*, 151; c) T. Kalwarczyk, N. Ziebacz, A. Bielejewska, E. Zaboklicka, K. Koynov, J. Szymanski, A. Wilk, A. Patkowski, J. Gapinski, H. J. Butt, R. Holyst, *Nano Lett.* **2011**, *11*, 2157; d) S. Yordanov, A. Best, H. J. Butt, K. Koynov, *Optics Express* **2009**, *17*, 21149.
[12] a) S. A. Sukhishvili, Y. Chen, J. D. Muller, E. Gratton, K. S. Schweizer, S. Granick, *Nature* **2000**, *406*, 146; b) J. Zhao, S. Granick, *J. Am. Chem. Soc.* **2004**, *126*, 6242; c) L. F. Zhang, S. Granick, *Proc. Natl. Acad. Sci. USA* **2005**, *102*, 9118; d) J. Donsmark, C. Rischel, *Langmuir* **2007**, *23*, 6614; e) S. Chiantia, J. Ries, P. Schwille, *Biochim. Biophys. Acta—Biomembranes* **2009**, *1788*, 225; f) A. Benda, V. Fagul'ova, A. Deyneka, J. Enderlein, M. Hof, *Langmuir* **2006**, *22*, 9580.
[13] B. D. Hughes, B. A. Pailthorpe, L. R. White, *J. Fluid Mech.* **1981**, *110*, 349.
[14] A. Goebel, K. Lunkenheimer, *Langmuir* **1997**, *13*, 369.
[15] S. Zeppieri, J. Rodriguez, A. L. L. de Ramos, *J. Chem. Eng. Data* **2001**, *46*, 1086.
[16] a) T. S. Horozov, R. Aveyard, B. P. Binks, J. H. Clint, *Langmuir* **2005**, *21*, 7405; b) D. Frydel, S. Dietrich, M. Oettel, *Phys. Rev. Lett.* **2007**, *99*; c) K. Masschaele, B. J. Park, E. M. Furst, J. Fransaer, J. Vermant, *Phys. Rev. Lett.* **2010**, *105*.
[17] a) R. C. Jeffrey, J. R. A. Pearson, *J. Fluid Mech.* **1965**, *22*, 721; b) K. Nagel, *Phys. Rev. E* **1996**, *53*, 4655.
[18] a) D. Aarts, M. Schmidt, H. N. W. Lekkerkerker, *Science* **2004**, *304*, 847; b) A. Braslau, M. Deutsch, P. S. Pershan, A. H. Weiss, J. Alsnielsen, J. Bohr, *Phys. Rev. Lett.* **1985**, *54*, 114; c) M. Perlin, W. W. Schultz, *Annu. Rev. Fluid Mech.* **2000**, *32*, 241.

Received: September 2, 2011
Published online: November 10, 2011

